Injectable oxygen liberating hydrogels increase survival and innervation of neural stem cell grafts prior to vascularization

Yi Wang
ANU
Jacob Thomas
Australian National University https://orcid.org/0000-0002-7406-8521
Nansook Hong
Australian National University https://orcid.org/0000-0002-7997-7687
Li Lynn Tan
Australian National University https://orcid.org/0000-0003-0606-4446
Duncan McGillivray
University of Auckland https://orcid.org/0000-0003-2127-8792
Adam Perriman
University of Bristol
Niamh Moriarty
Florey Institute of Neuroscience
Clare L Parish
Florey Institute of Neuroscience and Mental Health
Richard Williams
Deakin University https://orcid.org/0000-0003-3831-8738
Colin Jackson (colin.jackson@anu.edu.au)
Australian National University https://orcid.org/0000-0001-6150-3822
David Nisbet
Australian National University https://orcid.org/0000-0002-1343-0769

Article

Keywords:

Posted Date: June 1st, 2022

DOI: https://doi.org/10.21203/rs.3.rs-50947/v1

Injectable oxygen liberating hydrogels increase survival and innervation of neural stem cell grafts prior to vascularization

Y. Wang[1], J.W. Thomas[1], N. Hong[2], L. L. Tan[2], D. J. McGillivray[3], A. W. Perriman[4], N. Moriarty[5], C.L. Parish[5], R.J.Williams[6], C.J. Jackson*[2], D.R. Nisbet*[1]

[1]Laboratory of Advanced Biomaterials, Research School of Electrical, Energy and Materials Engineering, Australian National University, Canberra, ACT 2601, Australia

[2]Research School of Chemistry, Australian National University, Canberra, ACT 2601, Australia

[3] School of Chemical Sciences, University of Auckland, Private Bag 92019, Auckland 1142, New Zealand.

[4] School of Cellular and Molecular Medicine, University of Bristol, Bristol, Bristol BS8 1TD UK

[5] The Florey Institute of Neuroscience and Mental Health, The University of Melbourne, Parkville, Victoria, Australia, 3052

[6] Centre for Molecular and Medical Research, School of Medicine, Deakin University, Warun Ponds, VIC 3216, Australia

Injectable hydrogels have great potential for use in regenerative medicine as cellular delivery vectors. However, as with other cell-laden transplantable materials, they suffer from issues relating to hypoxia, including poor cell survival, differentiation, and functional integration owing to the lack of an established vascular network. Here, we have engineered a hybrid myoglobin:peptide hydrogel that can concomitantly deliver stem cells and oxygen to the brain to support engraftment until vascularisation can occur naturally. This hybrid hydrogel can modulate cell fate specification within progenitor cell grafts, resulting in a significant increase in neuronal differentiation. The addition of myoglobin to the hydrogel resulted in more extensive innervation within the host tissue from the grafted cells, which is essential for neuronal replacement strategies to ensure functional synaptic connectivity. Further development of this approach could result in greater functional integration of stem cell-derived grafts for the treatment of neural injuries and diseases affecting the central and peripheral nervous systems.

Introduction

Injectable biomaterials that can deliver, support, and integrate stem cells hold significant promise for tissue regeneration, as they can easily be administered to the site of therapeutic need where they rapidly and effectively fill voids to ensure good tissue contact. However, due to their injectable nature and the general lack of vascularization at the site of injection, they rely on diffusion of oxygen through the tissue to the site of the graft. This is a significant limitation, particularly during the important early stages before natural angiogenesis mechanisms have begun[1-4]. Indeed, it has been shown that neuronal survival is reduced within a hypoxia or ischemia milieu[5]. While low oxygen levels (below 2%) can lead to cell death, it is apparent that high levels of oxygen may also induce destructive effects[6, 7]. Finally, beyond the need for oxygen for respiration and energy production, it is also apparent that it is an important signalling molecule for processes such as apoptosis and differentiation in CNS cell precursors[8]. It is understood that the major contributor to oxidative stress within the brain is elevated levels of intracellular ROS[9], which have been shown to promote apoptosis in oligodendrocytes and other CNS derivatives[10]. Altogether, it is clear that homeostasis of oxygen levels within an ideal range is critical for the survival, proliferation, and differentiation of neuronal progenitor cells[7, 11].

Oxygen-releasing biomaterials have emerged as a new paradigm for the non-vascular support of cell metabolism within novel engineered tissue *in vitro* and *in vivo*[12-14]. While much of the attention has focused on the use of hydrogen peroxide (H_2O_2) for controlled and prolonged oxygen delivery[15], it has been recognised that the presence of H_2O_2 may result in increased production of free radicals[13], although this can be overcome to some extent via the incorporation of enzymes such as catalase multicomponent systems[14, 16]. An alternative approach, which has been used to stimulate oxygenation of stem cells during the engineering of cartilage tissue[17, 18], is to utilize oxygen binding proteins, such as myoglobin (Mb), to transport oxygen directly to the tissue. Mb natively facilitates oxygen transport along partial pressure of oxygen (PO_2) gradients and serves as an oxygen reservoir, binding oxygen via the prosthetic heme group in high oxygen concentrations (oxymyoglobin), and releasing oxygen in hypoxic conditions (deoxymyoglobin), such as those experienced during periods of increased metabolic activity[12, 19]. Moreover, during hypoxic or anoxic conditions, Mb scavenges potentially cytotoxic reactive oxygen species (ROS), such as peroxide and nitric

oxide, which are by-products of oxygen metabolism[20]. These homeostatic properties make Mb an ideal O_2 vector/reservoir for stem cell grafts.

Although proteins, such as Mb, have significant potential in improving cell transplantation outcomes, they cannot be simply injected into the specific site of a stem cell graft to influence cell fate, as they are rapidly degraded and diffuse away from the focal site, and instead required continual infusion[21-23]. Thus, innovations to allow protein delivery and ensure physiologically relevant *in vivo* presentation and long-term activity are required. Substantial progress has been made in this area by generating hybrid protein:peptide hydrogels; for example, we recently demonstrated that brain derived neurotrophic factor (BDNF) could be kinetically stabilised[24], increasing its active presentation duration from *ca*. 15 mins to 28 days. Mb has been studied in this context, where it has been imbibed[25] or immobilised within sol/gel films[17, 25]. In contrast to covalent protein immobilization strategies that require chemical modifications, we have recently shown that the use of non-covalent electrostatic protein:hydrogel interactions under mild conditions can allow for substantial active protein retention within biocompatible peptide hydrogels for long durations[26].

Here, we hypothesised that a hydrogel that can bind and release oxygen and scavenge ROS *via* the incorporation of myoglobin could be applied to the site of the graft to dramatically improve the efficacy of stem cell grafting technology within the central nervous system (CNS). In this work, we describe the synthesis of a multifunctional oxygen-responsive hydrogel that is capable of enhancing the delivery and promoting the long-term survival and integration of grafted neural stem cells in the brain, demonstrating that this approach is simultaneously capable of enhancing the delivery and promoting the long-term survival and integration of grafted cortical neural stem cells. Importantly, these results were achieved within hostile brain tissue post iatrogenic injury. Histological analysis at 28 days post *in vivo* delivery revealed significantly enhanced survival and differentiation of grafted neuronal stem cells towards mature neurons, compared with a myoglobin-free hydrogel. We observed extensive innervation of the endogenous tissue in the presence of myoglobin, providing the first evidence of the importance of incorporating bioinspired oxygen delivery within a functional hydrogel to synergistically promote the long-term survival and integration of stem cell transplants. This represents a generalizable strategy for the development of tissue mimetic, readily injectable nanomaterials that have diverse applications, including in cell transplantation, gene and drug delivery, 3D *in vitro* disease models and organ on a chip technology.

Results

Peptide-based nanoscaffolds sustain myoglobin and subsequently oxygen delivery. In order to develop an oxygen vector capable of accelerating stem cell therapies, we optimised a previously described peptide hydrogel, demonstrating its capability for delivering oxygen *via* myoglobin within an infarct injury. In this study, we presented the functional epitope encoded for the binding domain of laminin (Fmoc-DD***IKVAV***) in high density on the surface of the nanofibrillar molecular hydrogel substructure[24, 27, 28]. This epitope was chosen due to its ability to promote neural adhesion, proliferation, differentiation, and plasticity[29]. We have previously demonstrated that this peptide spontaneously self-assembles into a hydrogel via π-β assembly and amphiphilic re-organisation[30]. Here, we investigated whether this self-assembly is adversely affected by the addition of purified Mb (*Equus caballus*) to the peptide precursor immediately before gelation, leading to a final mass ratio of 1:15 Mb:peptide. This yielded characteristically red-colored hydrogels, which were then optimised to be compliance matched to that of the rodent brain ($G' \approx 100$ Pa, $G'' = 100$ Pa) (Supplementary Information Figure S1).

The addition of Mb resulted in minimal changes in the biophysical properties of the hydrogel as determined by transmission electron microscopy (TEM), Fourier transform infrared spectroscopy (FTIR), and circular dichroism (CD) (Figure 1A-D). These results indicated that the system undergoes two component assembly, where myoglobin molecules associate with the surface of, but do not disrupt the structure of, the nanofibrils. SAXS analysis of the hydrogel and myoglobin:hydrogel samples confirmed this (Supplementary Information Figure S2). Both samples exhibited classic hydrogel SAXS scattering profiles, with a slope that is consistent with randomly oriented fibres. Weak features present at ~0.16 $Å^{-1}$ and 0.27 $Å^{-1}$ in both samples, indicating similar cluster sizes in both of the the hydrogels. As these features are present in both the hydrogel and myoglobin:hydrogel samples, this indicates that the base structure of the self- assembled peptide (SAP) hydrogel is unaffected by the myoglobin. There is a slight difference between the two samples, with additional scattering visible between 0.01 $Å^{-1}$ - 0.15 $Å^{-1}$ in the hydrogel:myoglobin sample, which is consistent with the scattering of myoglobin. Overall, this demonstrates that the network morphology underpinning the hydrogel is not affected by the myoglobin and the data was consistent with a gel in which myoglobin molecules are loosely associated with the surface of the nanofibrils.

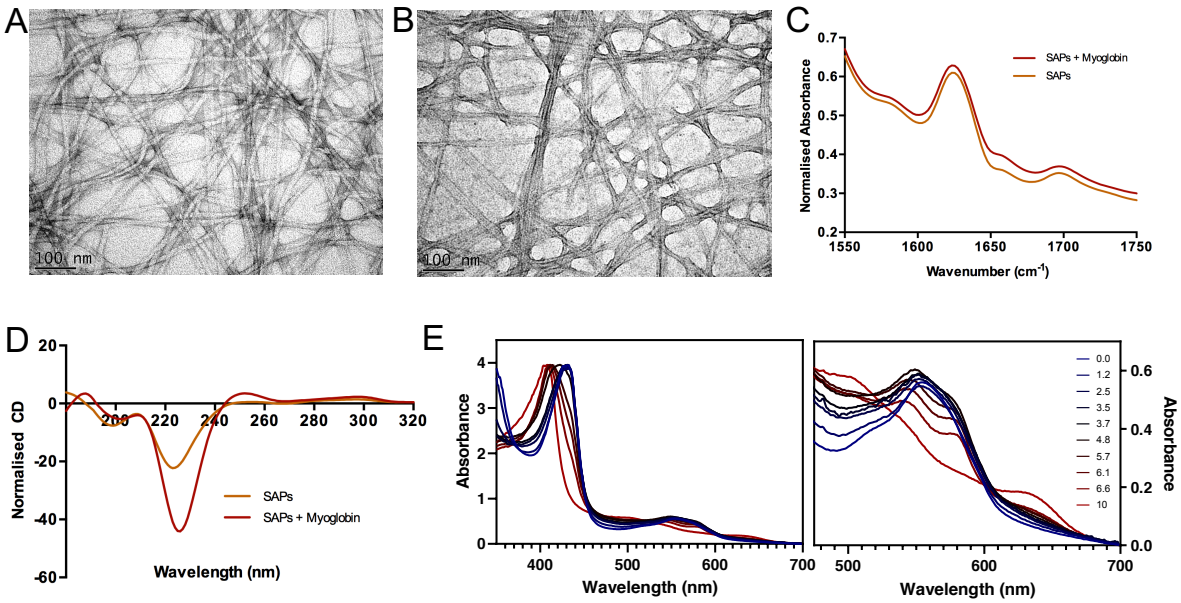

Figure 1. Biophysical and biochemical characterization of the hydrogel and myoglobin:hydrogel hybrid material. Representative TEM images of the hydrogel (Fmoc-DDIKVAV) in the absence (A) and presence (B) of myoglobin. (C) FTIR spectra and (D) CD absorbance spectra of the hydrogel with and without myoglobin. (E) Functional analysis of the hydrbid myoglobin:hydrogel over a 10 hour period, showing the gradual oxygenation and oxidation of myoglobin within the gel. Metmyoglobin (oxidized) is identifiable by a small peak at 628 nm, reduced absorbance between 550-600 nm, and a shift in the maximum absorbance from 426 to 409 nm.

The effect of the gel association on the O_2-binding of myoglobin was investigated over 10 hours using UV-vis spectroscopy[31] (Figure 1E). The hydrogel containing no myoglobin displayed limited absorption throughout the wavelength range, as expected. The reduced deoxymyoglobin spectra at $t = 0$ exhibited a characteristically intense Soret band at 426 nm[32]. The full transition from reduced deoxymyoglobin to oxymyoglobin to oxidized myoglobin (metmyoglobin), observable by an intense band at ~409 nm and a weaker Q-band at 628 nm, took place over the course of 10 hours. The observation of these spectral changes, which are the same as those observed during the oxidation of normal myoglobin in solution (Supplementary Information Fig. S3), demonstrate that myoglobin is incorporated within the hydrogel in a functional state. Interestingly, the rate of oxidation within the hydrogel was substantially slower than what was observed in the absence of the hydrogel, which suggests that the oxygen diffusion coefficient of the hydrogel is lower, which is consistent with previous studies of oxygen diffusion through hydrogels[33].

Myoglobin-functionalisation of nanoscaffolds demonstrates *in vivo* biocompatibility. Next, we investigated the capacity of our hydrogels to act as novel oxygen vectors to support host tissue post administration. To do this, firstly we explored the most important aspect of any synthetic implant, the biocompatibility of the hydrogel oxygen vectors within the host brain, determining how myoglobin functionalisation and oxygen delivery impacted the host immune response. The resultant peptide/protein concentration of 10 mg mL^{-1} was administered through ultrafine glass capillaries into the brain. At 28 days post administration, neither the Fmoc-DDIKVAV peptide hydrogel, nor the hydrogel functionalised with myoglobin, showed any detrimental impact (i.e no increase in local immune-responsive cells). This was determined through examination of the density of proinflammatory GFAP+ astrocytes immediately adjacent to the site of hydrogel administration within the brain, where no increase in the number of reactive astrocytes was observed (Figure 2). Importantly, we have recently shown in the stroke injured brain that an unfunctionalized IKVAV SAP hydrogel has no influence on the immune system with the same density of reactive astrocytes and microglia compared to sham (saline) injected controls[24].

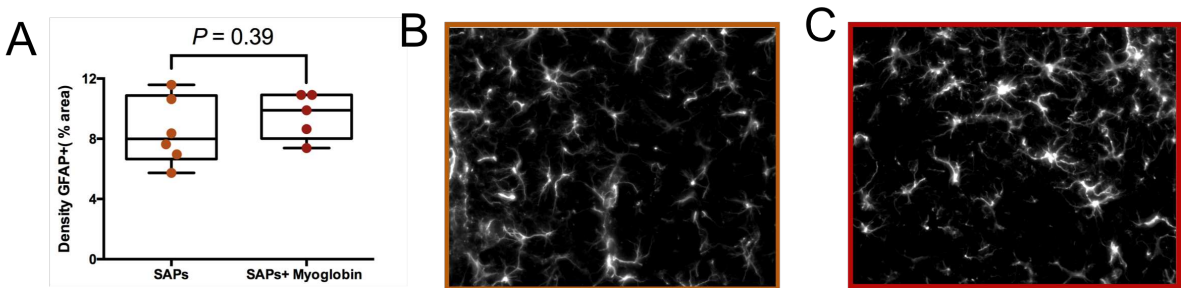

Figure 2: Myoglobin had no effects on the host inflammatory response. A: Density of GFAP+ reactive astrocytes surrounding the GFP^+ graft. B&C: Representative images of GFAP+ immunolabeling adjacent to GFP+ graft in SAPs and SAPs+Myoglobin groups, respectively. Data represents mean ± standard error of the mean (SEM).

Sustained oxygen delivery from protein-inspired nanoscaffolds concomitantly provides physical and trophic support to transplanted cortical progenitor cells. Having established that the Mb-functionalised hydrogel is biocompatible, we then investigated the effect of Mb on the survival and differentiation of transplanted progenitor cells. We encapsulated green fluorescent protein reporter (GFP+) neuronal progenitor cells within the peptide hydrogel (+/-myoglobin) for co-delivery into the brain. The GFP reporter within the cells enables clear identification of transplanted cells and their neuronal processes within the host brain tissue.

Using GFP to delineate the graft core, we observed a significantly increased graft volume ($p = 0.029$), when Mb was incorporated within the hydrogel *vs.* the no-Mb control (Figure 2).

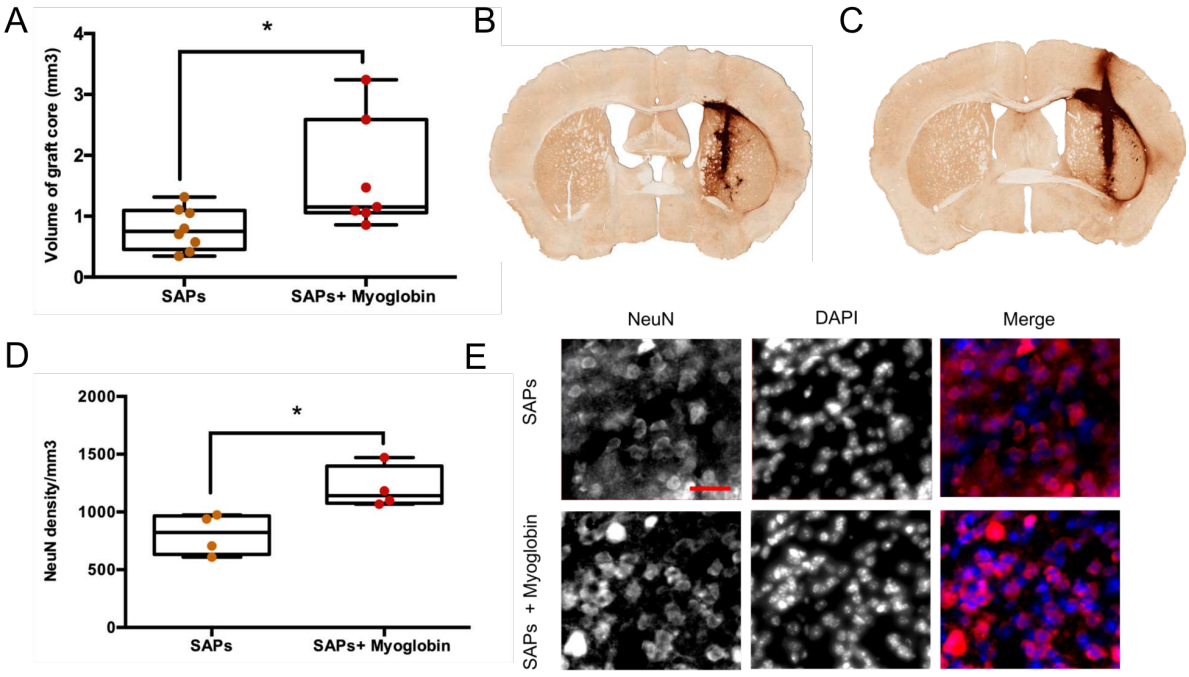

Figure 3: Incorporation of myoglobin within SAPs improves graft survival and neuronal differentiation. A: Volume of graft core. B&C: Representative photomicrographs providing a coronal view of GFP+ graft in SAPs and SAPs+Myoglobin groups, respectively. D:Density of NeuN+ in graft. E: Representative images showing the NeuN+ (red), DAPI expression (blue). Data represents mean ± standard error of the mean (SEM). Scale bar represents 200 μm.

While the increased cell survival and graft core volume observed in the SAP:myoglobin data is beneficial, the ability to replace relevant neuronal circuity/cell types that have been damaged or lost is more important for the treatment of brain injury[34]. To this end, the generation of new neurons within the graft is essential and is the primary motivation to increase oxygen supply within the donor tissue. To investigate the effect of Mb on cell differentiation, we quantified the density of NeuN+ cells within the graft 28 days post transplantation. Previously, we have demonstrated that our IKVAV epitope-containing hydrogel scaffolds are capable of increasing the proportion of neurons within the graft because the high availability and surface density of the IKVAV epitope in the SAP promotes neuronal adhesion, differentiation and axonal growth of neural progenitors more efficiently than laminin itself[24, 29, 35]. The IKVAV epitope-containing hydrogel resulted in a density of neurons of 807 ± 89 cells/mm^3 within the graft core (Figure 3). Remarkably, we observed an additional significant increase ($p=0.02$) in

neuronal differentiation to a density of 1205 ± 92 cells/mm^3 as a result of the sustained delivery of oxygen *via* myoglobin (Figure 3). As the base hydrogel structures are identical (Figure 1), this suggests that the presence of myoglobin within the hydrogel can not only enhance the delivery and long-term survival of grafted cortical neural stem cells, but also bias their differentiation towards the neuronal fate that is critical for circuity repair and reconstruction. In addition to its biological functionality, this also exemplifies this facile method for the creation of a hydrogel oxygen vector using the immobilisation, of myoglobin for the controlled release of oxygen *in vivo*.

In light of the enhanced neuronal differentiation observed due to the presence of Mb in the SAP hydrogel, we subsequently investigated the ability of cells to integrate into the host brain, as an indicator of brain repair. Graft integration was assessed at 28 days post administration by volumetric analysis of the GFP+ fibres within the surrounding brain parenchyma. These results showed that the transplanted GFP+ progenitors were capable of integrating into the host tissue, with extensive GFP+ fibre growth observed surrounding the graft core and innervating the host tissue (Figure 4). Again, there was a statistically significant increase in innervation volume ($p=0.0009$) in the Mb:SAP hydrogel over the SAP hydrogel without Mb, increasing almost 2-fold from 3.3 ± 0.4 mm^3 to 6.1 ± 0.5 mm^3. This is important, as it suggests axonal growth from cells delivered within the peptide hydrogel was not impeded post neuronal differentiation and that the delivery of oxygen within the graft core did not result in GFP+ fibres being restricted within the graft core. This is evidenced by the fact that the same GFP+ fibre density was observed within the parenchyma both with and without myoglobin functionalisation (Figure 3). Furthermore, we observed doublecortin (DCX+) migrating neuroblasts at both the edge of the grafts and within the surrounding parenchyma, similarly demonstrating that the presence of the hydrogel scaffold (or formation of host scar tissue) did not impede grafted cell migration and integration within the host brain (Figure 5). Therefore, myoglobin functionalisation of the hydrogel resulted in enhanced integration of neural stem cell grafts into existing host parenchyma. This demonstrates the importance of engineering multicomponent nanoscaffolds to advanced regenerative outcomes, which in this case was achieved *via* the incorporation of oxygen delivery within a functional hydrogel to synergistically promote the long-term survival and, importantly, the integration of stem cell transplants within the host brain.

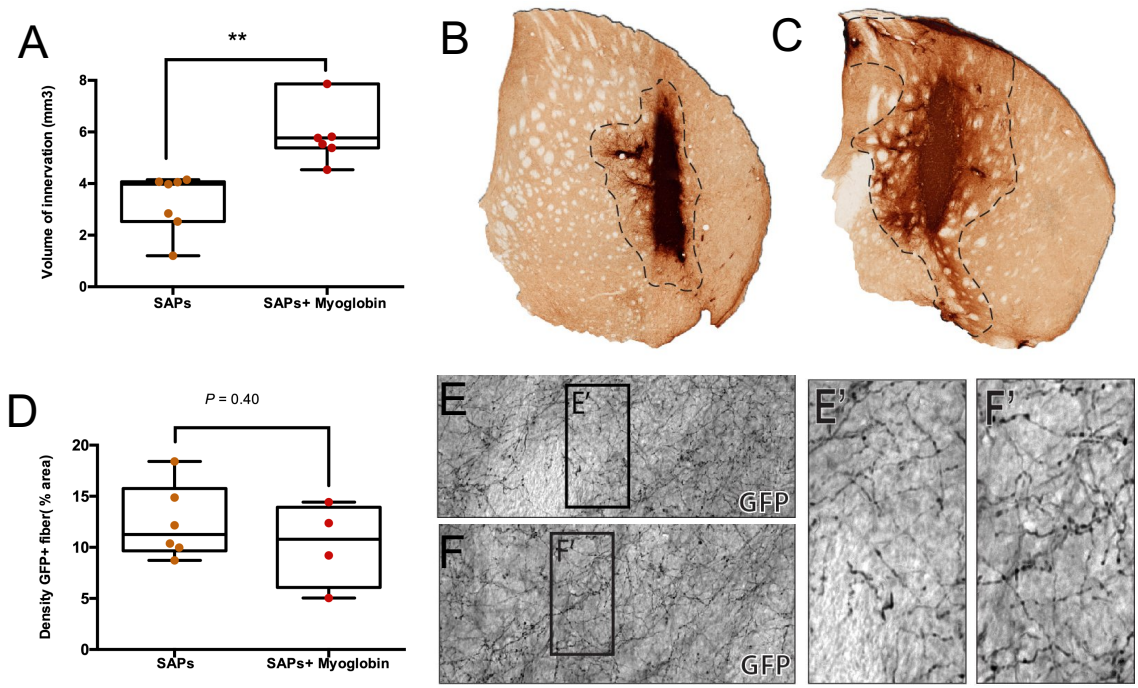

Figure 4: myoglobin incorporated within SAPs promotes the graft innervation. A: Volume of innervation. B&C: Representative photomicrographs providing innervation of GFP^{+} graft in SAPs and SAPs+Myolobin groups. D: Density of GFP fibre. E & E' present the GFP fibre high magnification in SAPs group. F & F' present the GFP fibre high magnification in SAPs+Myoglobin group. Data represents mean ± standard error of the mean (SEM).

We further assessed the grafts for evidence of excessive cell proliferation 28 days post implantation using the expression of Ki67 to mark cells undergoing proliferation[36]. Excessive proliferation was not observed, with the density of Ki67+ cells being the same between the functionalised and unfunctionalized hydrogels (Figure 5). These Ki67+ cells are closely associated with blood vessels and may be endothelial progenitor cells undergoing angiogenesis within the graft tissue to form new blood vessels[24, 37]. Taken together, these *in vivo* data suggest the incorporation of myoglobin in a SAP hydrogel can synergistically promote the long-term survival and, importantly, the integration of stem cell transplants within the host brain, whilst avoiding undesirable cell fates and immune responses.

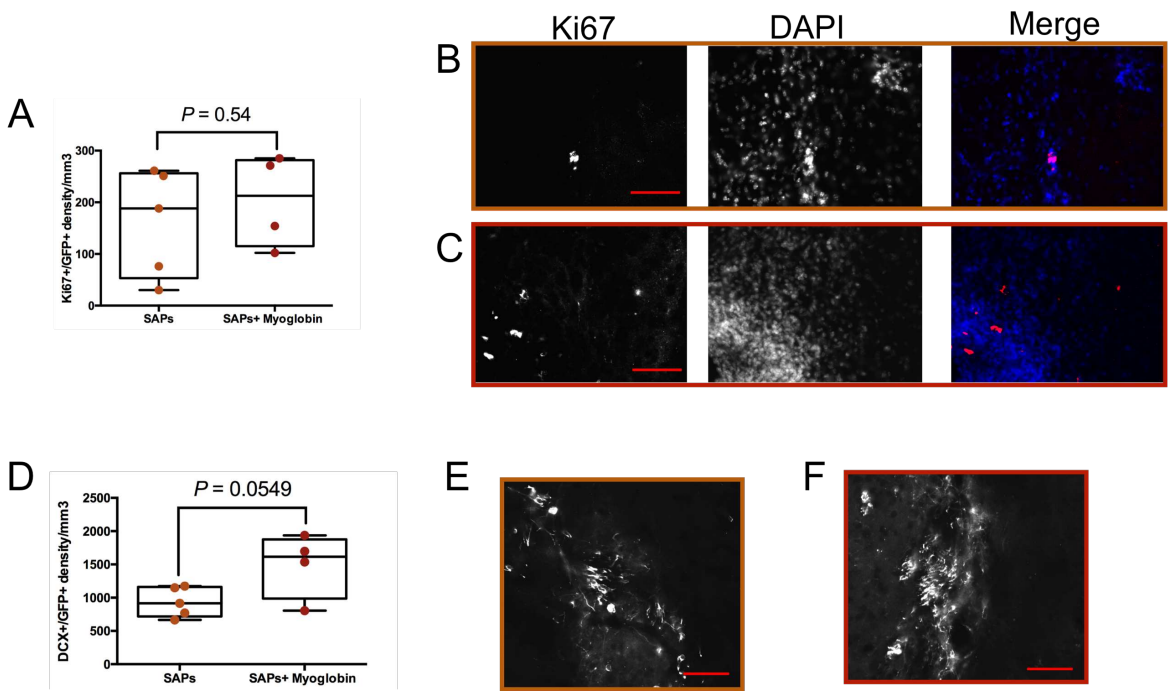

Figure 5: Myoglobin has no effects on proliferation compared to SAPs alone. A: Density of Ki67$^+$ proliferative cells in the graft. B&C: Representative images of Ki67$^+$ immunolabeling in the graft in SAPs and SAPs+Myoglobin groups, respectively. D: Density of DCX$^+$ migrating cells in the graft. E, F: Representative images of DCX$^+$ immunolabeling in the graft in SAPs and SAPs+Myoglobin groups, respectively. Data represents mean ± standard error of the mean (SEM). Scale bar represents 50 µm.

Discussion

The future success of cell transplantation technologies will depend on the ability to improve upon current deployment methods to increase implanted cell survival, while also providing a suitable milieu for the deployed cells to differentiate and integrate within the host circuitry[1, 38]. To achieve this, cellular microenvironments must be engineered that are capable of chemically and physically supporting the survival, differentiation, and neuronal connectivity of transplanted cells[2]. We have recently developed a new class of programmed peptide that fulfils such requirements[28, 35, 39]. We have investigated their capacity as adjuvants for cell transplantation in brain repair, due to their ability to mimic aspects of brain tissue via the high-density presentation of the functional epitope from laminin (IKVAV), which promotes tissue regeneration and supports cells during all stages of transplantation[27, 37]. We have also demonstrated the unprecedented ability of our transplantation vector to protect fragile therapeutics to provide a standardised and supportive milieu unlike the unpredictable injury environment[24, 28]. However, this delivery system still faces problems, including poor survival

of cells within the core of large grafts, and difficult in promoting lineage specific differentiation, and the integration of grafted cells within the host tissue. Given the known issues related to oxygen diffusion through hydrogels and the general lack of vascularisation at the site of transplant, the inability to maintain appropriate oxygen homeostasis is one of the most pressing issues.

Here, we provide the first evidence that a peptide hydrogel containing oxygen carrier proteins, such as Mb, is capable of sustaining the *in vivo* delivery of oxygen to stem cells grafts, positively impacting their survival and integration, and modulating stem cell specification. This was achieved through exploiting the large surface area to volume ratio of the peptide nanofibrils that comprise our peptide hydrogel (Figure 1), which acted as a substrate for macromolecular self-association of myoglobin. We have previously demonstrated that this approach protects proteins from proteases, yet maintains their conformation and accessibility to interstitial fluids[24, 35]. In terms of the development of strategies to deliver oxygen *in situ*, it is important to note that the production of the SAP:myoglobin hydrogel did not compromise the function of either myoglobin or the hydrogel itself (Figure. 1). The increased cell survival, differentiation and integration/innervation that was observed in the SAP:myoglobin cell grafts is evidence that the presence of myoglobin was beneficial to transplantation. It is equally important to note that we did not observe any negative effects relating to the presence of myoglobin, such as excessive cell proliferation or immune responses.

This work poses two questions relating to the mechanism of how this oxygen-vector hydrogel is contributing to the improved stem cell graft survival, differentiation and integration that we have observed. The first relates to the role of the O_2 that is delivered to the cells from the hydrogel once the partial pressure of oxygen drops below a critical value. We hypothesise that the presence of myoglobin allows these hydrogels to act as a temporary 'bloodstream' for the grafted cells prior to adequate angiogenesis and vascularisation within the graft. We have observed host derived angiogenesis over time within large stem cell grafts previously[24, 37]. Indeed, the importance of oxygen in enhancing neuronal circuitry reconstruction to ensure functional synaptic connectivity with remote brain regions has been well documented (Figure 4)[7, 11]. The second question relates to the role of ROS scavenging by myoglobin. Previous work has indicated that myoglobin may act as a scavenger of ROS, such as peroxides and nitric oxide[40] (the by-products of oxygen metabolism) and that the presence of ROS promotes apoptosis in CNS deriviatives[10]. Thus, we hypothesize that the ROS scavenging ability of

myoglobin has ameliorated many of these deleterious effects of ROS within our stem cell grafts.

In summary, our results demonstrate that an oxygen liberating peptide hydrogel, capable of sustaining the *in vivo* delivery of oxygen to stem cells grafts, positively impacts cell survival, integration and differentiation. These results demonstrate the importance of engineering hybrid hydrogel systems, capable of concomitantly delivering stem cells with appropriate therapeutics, in this case oxygen, when attempting to promote tissue repair and reconstruction. Importantly, while proof-of-concept is demonstrated within the brain, this approach represents a rational and generalizable strategy for the development of readily injectable cell supportive nanomaterials for a diverse range of applications, including cell transplantation, gene and drug delivery, 3D *in vitro* disease models and organ on chip technology.

Methods

Preparation of self-assembling peptide scaffolds

Fmoc-DDIKVAV was synthesised at 0.4 mmol scale by solid phase peptide synthesis using a rotating glass reactor vessel. All chemicals were purchased from Sigma Aldrich (Australia) with the amino acids being purchased from Pepmic (China). The Fmoc-DDIKVAV hydrogel were prepared at a final concentration of 15 mg mL^{-1} using a well-established pH switch. Briefly, approximately 10 mg of peptide was dissolved in 200 µL of deionised water with 100 µL 0.5 M sodium hydroxide (NaOH). Then 0.1 M of hydrochloric acid (HCl) was added dropwise with continuous vortexing until the solution reached physiological relevant pH (Oaktron pH 700 micro pH electrode, Thermo Scientific). 0.01 M Phosphate buffered saline (PBS)[41] was added to final 15 mg mL^{-1} concentration of hydrogel. For *in vitro* use, Hank's buffered saline solution (HBSS) (Gibco) was used in place of the PBS.

Lyophilized horse skeletal muscle myoglobin (Sigma) was reconstituted in a PBS buffer and purified further by size exclusion using a SEC200 26/600 column (GE Healthcare) and an AKTA FPLC (GE Healthcare). The protein eluted in a single peak and no additional protein bands were visible on SDS-PAGE. The purified protein was aliquoted into 500 µL samples before being freeze-dried and stored at -80 °C. For the preparation of the myoglobin:hydrogel hybrid, 1.2 mg of myoglobin was solubilised in 90.09 µL PBS as the stock solution, then 50

μL of this sample was added into the hydrogel (prepared as described above) to a final concentration of 1 mg mL^{-1} myoglobin. The vial was vortexed (30 seconds) for homogenisation and rested (60 seconds) for re-gelation. The final hydrogel contained 15 mg mL^{-1} peptide hydrogel and 1 mg mL^{-1} myoglobin.

Spectral characterisation of myoglobin-functionalised hydrogels

Unfunctionalized Fmoc-DDIKVAV hydrogel (15 mg mL^{-1}) and the same hydrogel functionalized (as above) with a final concentration of 1 mg mL^{-1} myoglobin that was already reduced by reaction with excess sodium dithionite ($Na_2S_2O_4$; 17 mM) were prepared in a N_2-containing anaerobic hood. Upon removal from the anaerobic hood, UV-Vis absorbance of the samples was monitored using a 96-well plate reading Epoch spectrophotometer (Biotek) over ten hours over a range of 350-700 nm. The same experiment was performed with free myoglobin in solution, in which everything in the system was identical, except for the absence of the hydrogel.

Transmission Electron Microscopy (TEM)

Negative-staining transmission electron microscopy (TEM) was performed using a HITACHI HA7100 TEM with a LaB6 cathode at 125 kV (tungsten filament). Formvar-coated copper grids were prepared with electron glow discharge at 15 mA for 30 seconds. The formvar-coated side of grids was loaded with hydrogel for 30 seconds, washed with DI H_2O (20 μL), treated with urea-formaldehyde (UF, 20 μL), and finally immersed into UF drop for 30 seconds. Between each step, excess solution was blotted off using filter paper. Then, the grids were allowed to dry overnight before imaging in the TEM.

Fourier Transform Infrared Spectroscopy (FTIR)

Fourier transform infrared spectroscopy (FTIR) was performed using an Alpha Platinum Attenuated Total Reflectance (ATR) FTIR (Bruker Optics) to monitor interactions in Amide I region (1550 to 1750 cm^{-1}). Approximately 20 μL of peptide hydrogel was placed on the single reflection diamond. Absorbance scans were obtained for each peptide, and a background buffer scan subtracted.

Circular Dichroism (CD)

Circular dichroism (CD) was performed using a Chirascan CD Spectrometer (Applied Photophisics Limited) to determine the secondary structure of hydrogel. The hydrogel was diluted at 1:10 ratio of hydrogel and DI H_2O to reduce scattering effects. The diluted gel around 400 µL was added into the cuvette with a 10 mm pathlength. CD scans ranged from 180 nm to 320 nm with a step size of 0.5 bandwidths using a Chirascan CD spectrometer (Applied Photophysics Limited) and a baseline (DI H_2O) was subtracted. The resulting data were averaged and smoothed post-acquisition using Chirascan software.

Small angle X-ray scattering (SAXS)

SAXS was performed using SAXS/WAXS beamline at the Australian Synchrotron[42]. Measurements were taken using camera length 900 mm, time exposure 1 second, energy 12 keV and 5% flux. Samples (SAPs groups, SAPs+ Myoglobin groups) were prepared as detailed above 1 day before measurement and stored in Eppendorf vials. PBS buffer was loaded into a 1 mm glass capillary for background measurements. Each hydrogel sample was loaded into six of the same capillaries for measurement. Capillaries were loaded into a custom mount which can hold and move the capillaries in two dimensions, with Kapton film windows. 1 s exposures were taken for each hydrogel-loaded capillary at 10 different positions evenly spread along the 3 mm capillary length. The average of these positions was used for one capillary. Each group of 6 capillaries for each sample was further averaged and the PBS background subtracted using ScatterBrain. There was strong scattering from the Kapton windows centred at ~0.4 $Å^{-1}$, which marks the upper limit of the useable Q-range measured.

Rheology

The rheological analysis was performed using a Kinexus Pro+ Rheometer (Malvern) and rSpace software. Approximately 0.2 mL of hydrogel was placed on a 20 mm roughened plate (with solvent trap, Lower Geometry: PLS55 C0177 SS, Upper Geometry: PU20 SR1351 SS). The gap size was 0.2 mm, and multiple frequency sweeps were performed for frequencies ranging from 0.1-100 Hz with a 0.1% oscillatory strain at a constant required temperature (37°C). Each gel was allowed a minimum of 5 minutes to set before testing.

***In vivo* transplantation of cells with myoglobin**

All animal procedures and methods were conducted in accordance with the Australian National Health and Medical Research Council's published Code of Practice for the Use of Animals in Research and were approved by the Florey Institute of Neuroscience and Mental Health Animal Ethics Committee. Cells for transplantation were obtained from time mated mice expressing green fluorescent protein (GFP) under the β-actin promoter, which enable clear distinction of the grafted cells (GFP+) cells within the host brain. Cortical brain tissue was isolated from pups at embryonic day 14.5 (E14.5), dissociated and resuspended at 100,000 cells/µl until the time of surgery. Hydrogels were sterilized by UV lamp for 2 hours and stock myoglobin was filtered by syringe filters (0.2 µm). Cells and gels were mixed at a 1:1 ratio immediately prior to *in vivo* delivery[43].

Adult C57BL/6 mice (n=6) were anaesthetized with 2% isoflurane and placed in the stereotaxic frame. A craniotomy was performed and unilateral microinjections of cells and hydrogels (total 2 µl) were implanted into the host striatum (0.5mm anterior and 2mmlateral to Bregma, and 3mm below the surface of the brain). After 28 days, mice were killed by an overdose of sodium pentobarbitone (100 mg/kg) and transcardially perfused with warm saline followed by 4 % paraformaldehyde (PFA). Brains were removed, post-fixed for two hours in 4% PFA and cryo-preserved overnight in 30% sucrose solution. Brains were sectioned on the coronal plane using a freezing microtome (40 µm thickness, 1:10 series).

Immunohistochemistry & Quantification

Immunohistochemistry was performed on free-floating brain sections as previously described[37]. In brief, brain sections were washed and incubated in primary antibodies overnight at room temperature, including: rabbit anti-GFP (1: 20,000; Abcam), chicken anti-GFP (1: 20,000; Abcam), sheep anti-Ki67 (1:40, R&D Systems), goat anti-doublecortin(DCX) (1:1000, Santa Cruz), chicken anti-GFAP (anti-glial fibrillary acidic protein, 1:500, Dako), mouse anti-NeuN (1:1000;Abcam). The following day sections were rinsed and blocked in 5 % donkey serum for 20 minutes. Secondary antibodies for (i) direct detection were used at a dilution of 1:200—DyLight 488, 549 or 649 conjugated donkey anti-mouse, anti-sheep, anti-chicken or anti-rabbit (Jackson ImmunoResearch); and (ii) indirect with streptavidin-biotin amplification—biotin conjugated donkey anti-rabbit (1:500; Jackson ImmunoResearch) followed by peroxidase conjugated streptavidin (Vectastain ABC kit, Vector laboratories). Finally, fluorescently labelled sectioned were stained with 4', 6-diamidino-2-phenylindole (DAPI, 1:5000, Sigma-Aldrich) to enable visualisation of all cells. Sections were mounted onto gelatinized slides and

coverslipped. All fluorescent images were captured using a Zeiss Axio Observer.Z1 epifluorescence and bright images were obtained using a Leica DM6000 upright microscope.

Total number of NeuN, DAPI, Ki67 and DCX cells within the graft, as well as the density of NeuN+, Ki67+ and DCX+ cells in grafts were counted from images captured at 40X magnification and expressed as per mm^3. The density of graft-derived GFP^+ fibers as well as host-derived $GFAP^+$ density (assessed as % immunoreactive pixels) were assessed at the graft-host border, as previously described and analysed[24].

Statistical analysis

Results represent means ± standard error of the mean (SEM). Data were analyzed using Graph Pad Prism 6.0 by one-way ANOVA with Turkey post-hoc statistic testing. Differences at $P < 0.05$-0.01 were considered statistically significant.

References

1. Mitrousis, N., Fokina, A. & Shoichet, M.S. Biomaterials for cell transplantation. *Nat Rev Mater* **3**, 441-456 (2018).
2. Tuladhar, A. & Shoichet, M.S. Biomaterials driving repair after stroke. *Nat Mater* **17**, 573-574 (2018).
3. Nih, L.R., Gojgini, S., Carmichael, S.T. & Segura, T. Dual-function injectable angiogenic biomaterial for the repair of brain tissue following stroke. *Nat Mater* **17**, 642-651 (2018).
4. Åberg, N.D. et al. Circulating levels of vascular endothelial growth factor and post-stroke long-term functional outcome. *Acta Neurologica Scandinavica* **141**, 405-414 (2020).
5. Doherty, J. & Baehrecke, E.H. Life, death and autophagy. *Nat Cell Biol* **20**, 1110-1117 (2018).
6. Erecińska, M. & Silver, I.A. Tissue oxygen tension and brain sensitivity to hypoxia. *Respiration Physiology* **128**, 263-276 (2001).
7. Panchision, D.M. The Role of Oxygen in Regulating Neural Stem Cells in Development and Disease. *J Cell Physiol* **220**, 562-568 (2009).
8. Mohyeldin, A., Garzon-Muvdi, T. & Quinones-Hinojosa, A. Oxygen in stem cell biology: a critical component of the stem cell niche. *Cell Stem Cell* **7**, 150-161 (2010).
9. Rodriguez-Colman, M.J. et al. Interplay between metabolic identities in the intestinal crypt supports stem cell function. *Nature* **543**, 424-+ (2017).
10. Casaccia-Bonnefil, P. Cell death in the oligodendrocyte lineage: A molecular perspective of life/death decisions in development and disease. *Glia* **29**, 124-135 (2000).
11. Morrison, S.J. et al. Culture in reduced levels of oxygen promotes clonogenic sympathoadrenal differentiation by isolated neural crest stem cells. *J Neurosci* **20**, 7370-7376 (2000).
12. Armstrong, J.P.K. et al. Artificial membrane-binding proteins stimulate oxygenation of stem cells during engineering of large cartilage tissue. *Nat Commun* **6** (2015).
13. Gholipourmalekabadi, M., Zhao, S., Harrison, B.S., Mozafari, M. & Seifalian, A.M. Oxygen-Generating Biomaterials: A New, Viable Paradigm for Tissue Engineering? *Trends in Biotechnology* **34**, 1010-1021 (2016).
14. Suvarnapathaki, S., Wu, X., Lantigua, D., Nguyen, M.A. & Camci-Unal, G. Breathing life into engineered tissues using oxygen-releasing biomaterials. *NPG Asia Materials* **11**, 65 (2019).
15. Abdi, S.I.H., Ng, S.M. & Lim, J.O. An enzyme-modulated oxygen-producing micro-system for regenerative therapeutics. *International Journal of Pharmaceutics* **409**, 203-205 (2011).
16. Oh, S.H., Ward, C.L., Atala, A., Yoo, J.J. & Harrison, B.S. Oxygen generating scaffolds for enhancing engineered tissue survival. *Biomaterials* **30**, 757-762 (2009).
17. Burke, M. et al. Regulation of Scaffold Cell Adhesion Using Artificial Membrane Binding Proteins. *Macromolecular Bioscience* **17**, 1600523 (2017).
18. Armstrong, J.P. et al. Artificial membrane-binding proteins stimulate oxygenation of stem cells during engineering of large cartilage tissue. *Nat Commun* **6**, 7405 (2015).
19. Burmester, T., Weich, B., Reinhardt, S. & Hankeln, T. A vertebrate globin expressed in the brain. *Nature* **407**, 520-523 (2000).
20. Kamga, C., Krishnamurthy, S. & Shiva, S. Myoglobin and mitochondria: A relationship bound by oxygen and nitric oxide. *Nitric Oxide-Biol Ch* **26**, 251-258 (2012).

21. Bruggeman, K.F. et al. Temporally controlled growth factor delivery from a self-assembling peptide hydrogel and electrospun nanofibre composite scaffold. *Nanoscale* **9**, 13661-13669 (2017).
22. Bruggeman, K.F., Williams, R.J. & Nisbet, D.R. Dynamic and Responsive Growth Factor Delivery from Electrospun and Hydrogel Tissue Engineering Materials. *Adv Healthc Mater* **7** (2018).
23. Wang, T.Y. et al. Functionalized composite scaffolds improve the engraftment of transplanted dopaminergic progenitors in a mouse model of Parkinson's disease. *Biomaterials* **74**, 89-98 (2016).
24. Nisbet, D. et al. Shear containment of BDNF within molecular hydrogels promotes human stem cell engraftment and postinfarction remodeling in stroke. *Adv Biosyst* **2**, 1800113 (2018).
25. Castro-Forero, A., Jimenez, D., Lopez-Garriga, J. & Torres-Lugo, M. Immobilization of myoglobin from horse skeletal muscle in hydrophilic polymer networks. *J Appl Polym Sci* **107**, 881-890 (2008).
26. Campbell, E.C. et al. Hydrogel-Immobilized Supercharged Proteins. *Adv Biosyst* **2** (2018).
27. Horgan, C.C. et al. Characterisation of minimalist co-assembled fluorenylmethyloxycarbonyl self-assembling peptide systems for presentation of multiple bioactive peptides. *Acta Biomater* **38**, 11-22 (2016).
28. Maclean, F.L., Ims, G.M., Horne, M.K., Williams, R.J. & Nisbet, D.R. A Programmed Anti-Inflammatory Nanoscaffold (PAIN) as a 3D Tool to Understand the Brain Injury Response. *Adv Mater* **30** (2018).
29. Wang, Y. et al. Peptide Programmed Hydrogels as Safe Sanctuary Microenvironments for Cell Transplantation. *Advanced Functional Materials* **30**, 1900390 (2020).
30. Rodriguez, A.L., Parish, C.L., Nisbet, D.R. & Williams, R.J. Tuning the amino acid sequence of minimalist peptides to present biological signals via charge neutralised self assembly. *Soft matter* **9**, 3915-3919 (2013).
31. Schenkman, K.A., Marble, D.R., Burns, D.H. & Feigl, E.O. Myoglobin oxygen dissociation by multiwavelength spectroscopy. *Journal of Applied Physiology* **82**, 86-92 (1997).
32. Ghosh, K., Kumar, R., Kumar, K., Ratnam, A. & Singh, U.P. Reactivity of nitric oxide with ruthenium complexes derived from bidentate ligands: structure of a ruthenium nitrosyl complex, photoinduced generation and estimation of nitric oxide. *Rsc Adv* **4**, 43599-43605 (2014).
33. White, J.C., Godsey, M.E. & Bhatia, S.R. Perfluorocarbons enhance oxygen transport in alginate-based hydrogels. *Polymers for advanced technologies* **25**, 1242-1246 (2014).
34. Grade, S. & Götz, M. Neuronal replacement therapy: previous achievements and challenges ahead. *NPJ Regenerative medicine* **2**, 1-11 (2017).
35. Rodriguez, A.L. et al. Using minimalist self-assembling peptides as hierarchical scaffolds to stabilise growth factors and promote stem cell integration in the injured brain. *J Tissue Eng Regen M* **12**, E1571-E1579 (2018).
36. Miller, I. et al. Ki67 is a graded rather than a binary marker of proliferation versus quiescence. *Cell Rep* **24**, 1105-1112. e1105 (2018).
37. Somaa, F.A. et al. Peptide-based scaffolds support human cortical progenitor graft integration to reduce atrophy and promote functional repair in a model of stroke. *Cell Rep* **20**, 1964-1977 (2017).
38. Madl, C.M., Heilshorn, S.C. & Blau, H.M. Bioengineering strategies to accelerate stem cell therapeutics. *Nature* **557**, 335-342 (2018).

39. Li, R. et al. Coassembled nanostructured bioscaffold reduces the expression of proinflammatory cytokines to induce apoptosis in epithelial cancer cells. *Nanomedicine* **12**, 1397-1407 (2016).
40. Jurgens, K.D., Papadopoulos, S., Peters, T. & Gros, G. Myoglobin: Just an oxygen store or also an oxygen transporter? *News Physiol Sci* **15**, 269-274 (2000).
41. Chazotte, B. Labeling Golgi with fluorescent ceramides. *Cold Spring Harbor protocols* **2012** (2012).
42. Kirby, N.M. et al. A low-background-intensity focusing small-angle X-ray scattering undulator beamline. *Journal of Applied Crystallography* **46**, 1670-1680 (2013).
43. Wang, T.-Y., Forsythe, J.S., Nisbet, D.R. & Parish, C.L. Promoting engraftment of transplanted neural stem cells/progenitors using biofunctionalised electrospun scaffolds. *Biomaterials* **33**, 9188-9197 (2012).

Supplementary Files

This is a list of supplementary files associated with this preprint. Click to download.

- myoglobinSI.pdf